Supplementary

Appendix 1: the detailed method for making the correspondence analysis

The radiologic and pathologic correspondence analysis included four steps: matching, overlapping, delineating, and analyzing. Firstly, according to the outline of the tumor and the anatomic locations among vessels, bronchi, and tumor on the histologic section, the same section on TS-CT was found. Secondly, after the radiologic and pathologic sections were matched, the tumor and the solid component on TS-CT were outlined, and the tumor on the histologic section was outlined as well. According to the similar tumor outlines and anatomic locations of vessels and bronchi, the radiologic and pathologic sections were overlapped. The radiologic and pathologic images were scaled equally for the overlapping. Thirdly, after the radiologic and pathologic overlapping, the histologic image was made 90% transparent, then the outline of the solid component on TS-CT could been seen on the histologic image, and the solid component outline was delineated on the histologic image. Finally, histologic features were evaluated in the delineated solid region on the histologic section, prevalence of histologic subtypes were recorded. In addition, histologic features were evaluated in the other region of the tumor which was regarded as the GGO region, and prevalence of the histologic features were recorded as well (*Figure S1*).

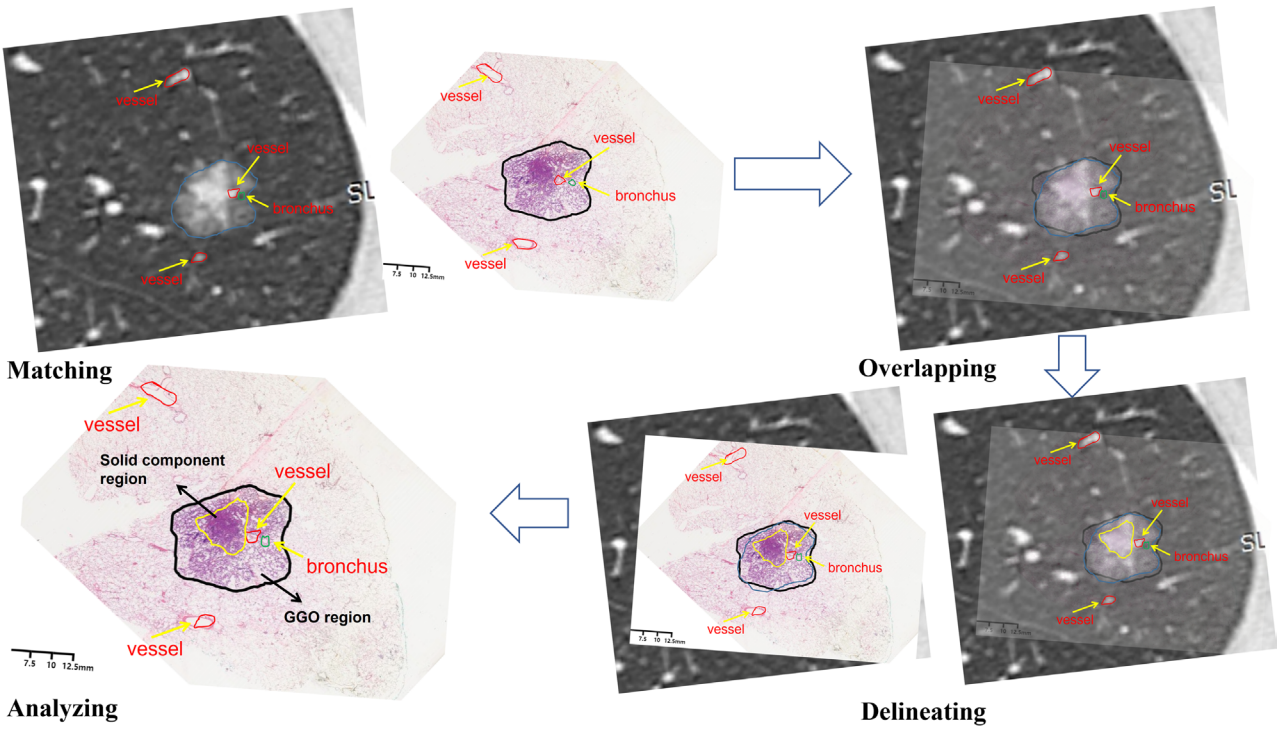

Figure S1 The process of the radiologic and pathologic correspondence analysis for the subsolid tumors including four steps: matching, overlapping, delineating, and analyzing.

https://dx.doi.org/10.21037/tlcr-2024-1063

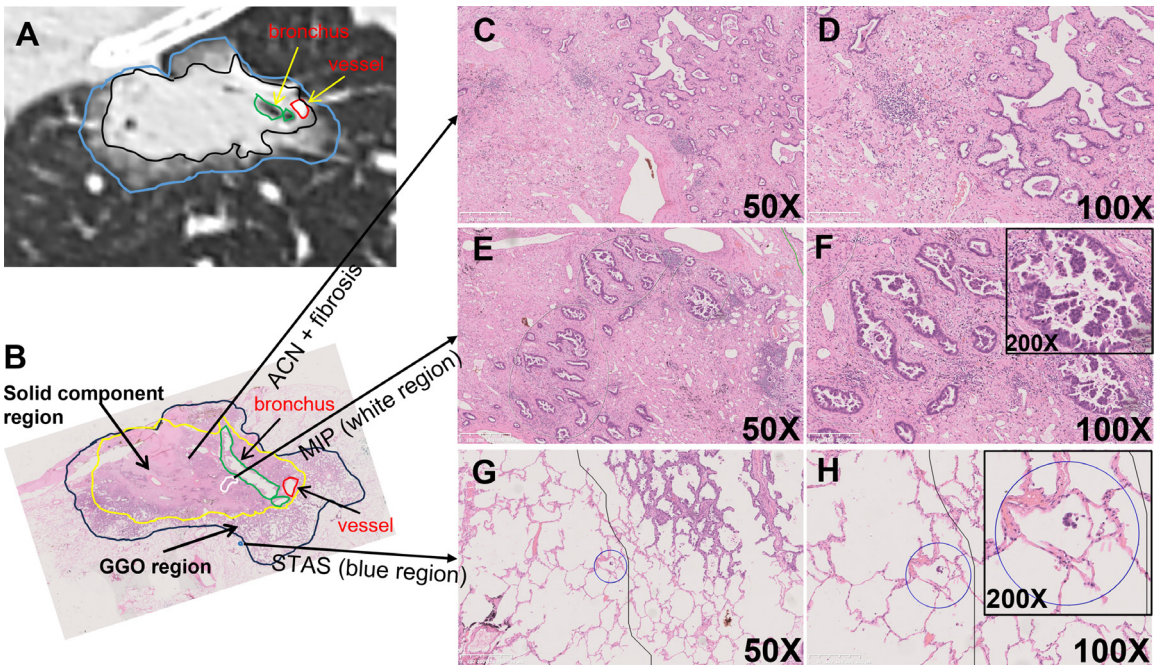

Figure S2 The histologic feature of one subsolid tumor with N2 disease. (A) One solid predominant tumor on TS-CT. (B) The matched pathologic section (yellow region was the radiologic solid component region). (C,D) The acinar subtype and fibrosis in the yellow region (original magnification: ×50 and ×100). (E,F) The micropapillary subtype in the yellow region (original magnification: ×50, ×100, and ×200). (G,H) The presence of STAS in the blue region (original magnification: ×50, ×100, and ×200). TS-CT, thin-section computed tomography.

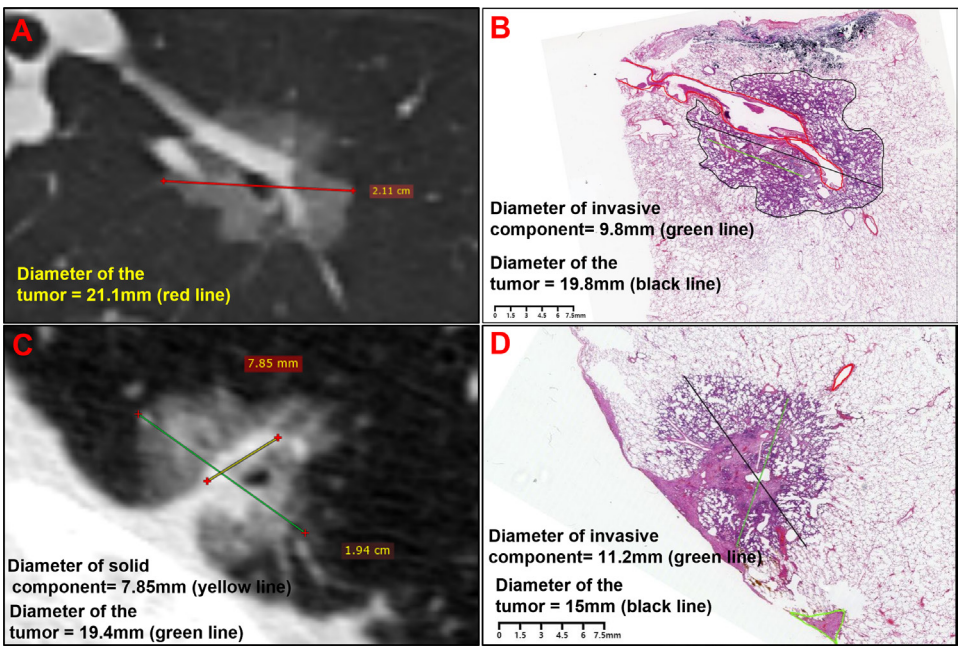

Figure S3 The comparisons of radiologic and pathologic tumor sizes and solid/invasive component sizes. (A) Measurement of the diameter of one pure GGO tumor on TS-CT. (B) Measurement of the diameter of tumor and invasive component on the matched pathologic section. (C) Measurement of the diameters of the tumor and solid component of one part-solid tumor on TS-CT. (D) Measurement of the diameter of pathologic tumor and invasive component on the matched pathologic section. TS-CT, thin-section computed tomography.

https://dx.doi.org/10.21037/tlcr-2024-1063

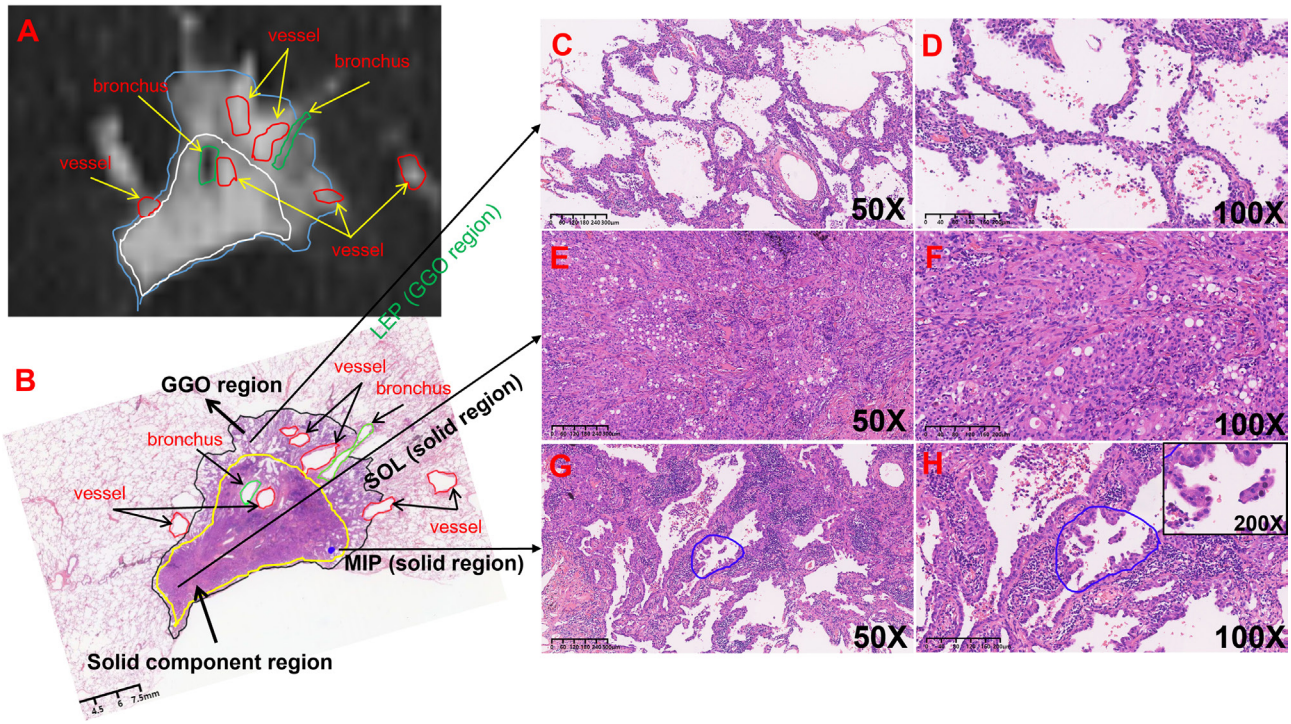

Figure S4 One subsolid tumor with pathologic solid subtype. (A) One solid predominant tumor on TS-CT. (B) The matched pathologic section (yellow region was the radiologic solid component region). (C,D) The LEP subtype in the GGO region (original magnification: ×50 and ×100). (E,F) The solid subtype in the yellow region (original magnification: ×50 and ×100). (G,H) The micropapillary subtype in the solid component region (blue region) (original magnification: ×50, ×100, and ×200). LEP, lepidic; TS-CT, thin-section computed tomography.

https://dx.doi.org/10.21037/tlcr-2024-1063

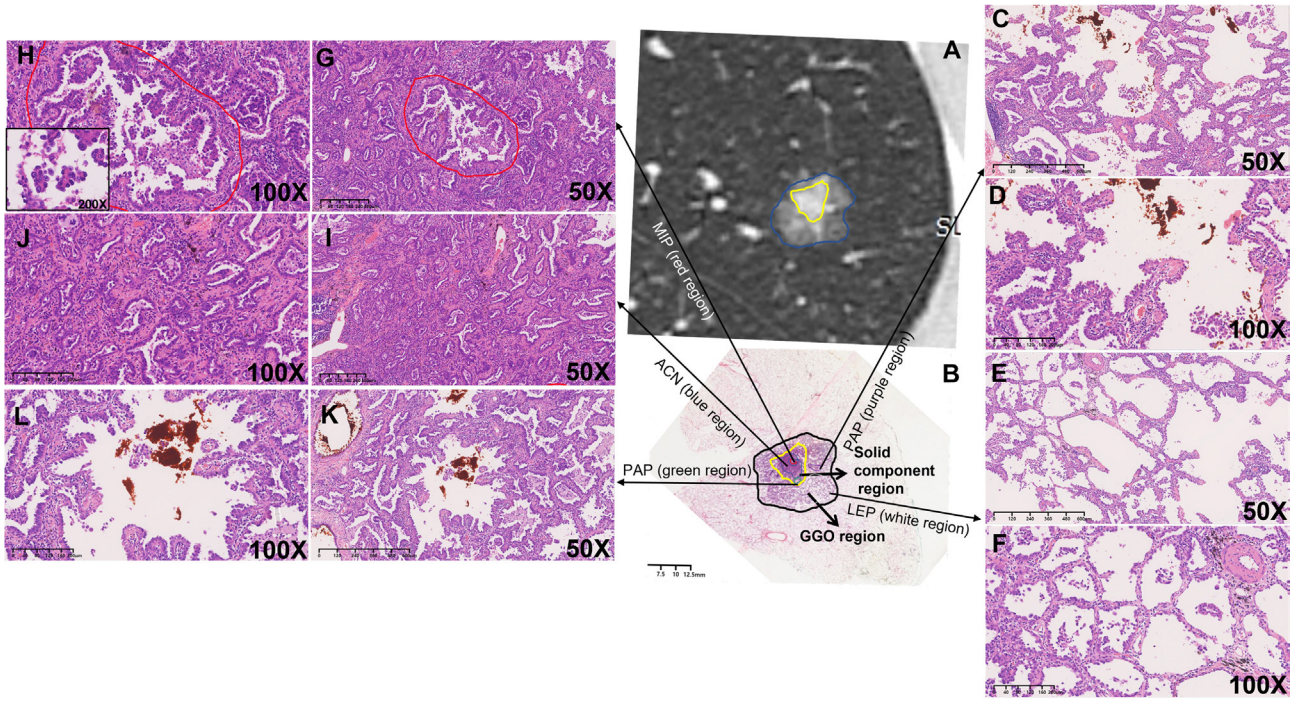

Figure S5 Distribution of histologic subtypes in the part-solid sections of part-solid tumors. (A) The part-solid section of one part-solid tumor on TS-CT. (B) the matched pathologic section (yellow region was the radiologic solid component region): the red region inside the yellow region was the MIP subtype; the blue region inside the yellow region was the ACN subtype; and the green region inside the yellow region was PAP subtype; the purple region was the PAP subtype; and the white region was the LEP subtype. (C,D) The papillary subtype in the GGO region (original magnification: ×50 and ×100). (E,F) The lepidic subtype in the GGO region (original magnification: ×50 and ×100). (G,H) The micropapillary subtype in the solid component region (original magnification: ×50, ×100, and ×200). (I,J) The acinar subtype in the solid component region (original magnification: ×50 and ×100). (K,L) The papillary subtype in the solid component region (original magnification: ×50 and ×100). MIP, micropapillary; ACN, acinar; PAP, papillary; LEP, lepidic; TS-CT, thin-section computed tomography.

https://dx.doi.org/10.21037/tlcr-2024-1063

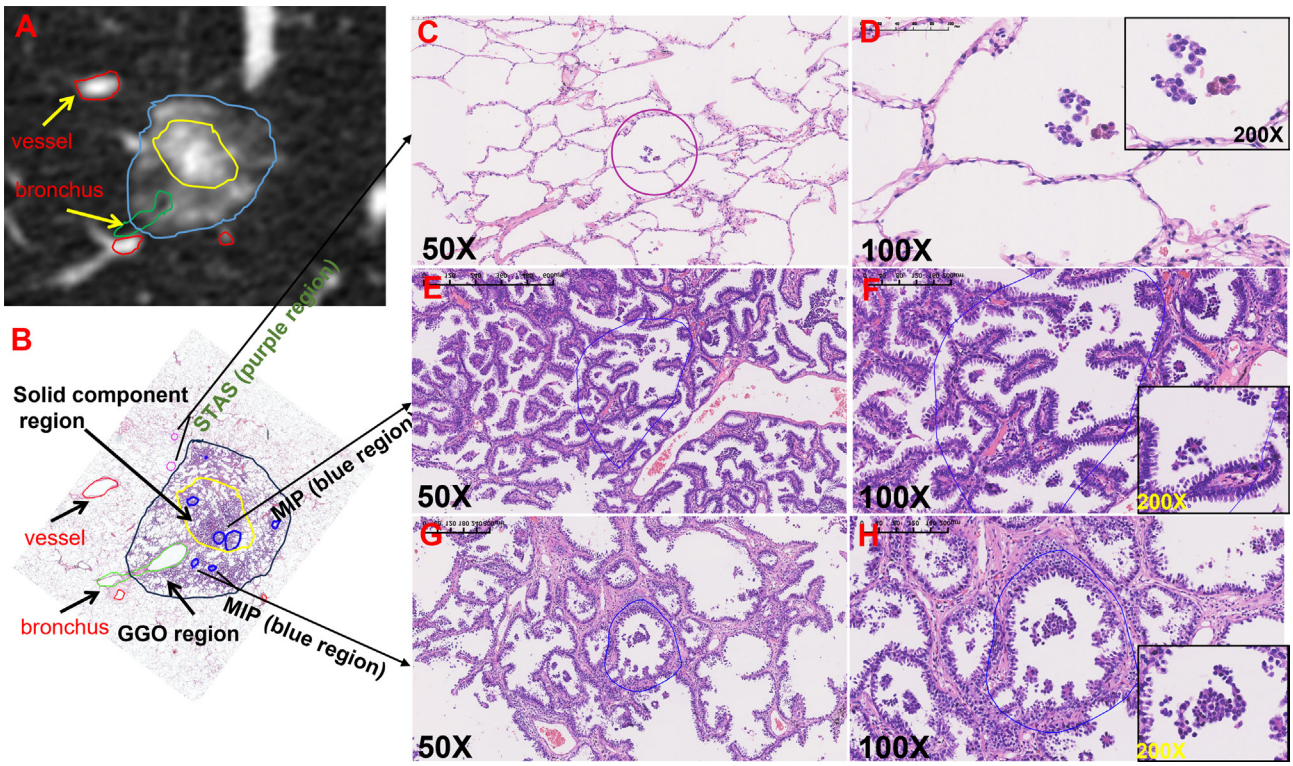

Figure S6 Distribution of the micropapillary subtype in the part-solid sections of part-solid tumors. (A) The part-solid section of one part-solid tumor on TS-CT. (B) The matched pathologic section (yellow region was the radiologic solid component region): the blue region was the MIP subtype. (C,D) The presence of STAS (purple region) (original magnification: ×50, ×100, and ×200). (E,F) The micropapillary subtype in the solid component region (original magnification: ×50, ×100, and ×200). (G,H) The micropapillary subtype in the GGO region (original magnification: ×50, ×100, and ×200). MIP, micropapillary; TS-CT, thin-section computed tomography.

https://dx.doi.org/10.21037/tlcr-2024-1063

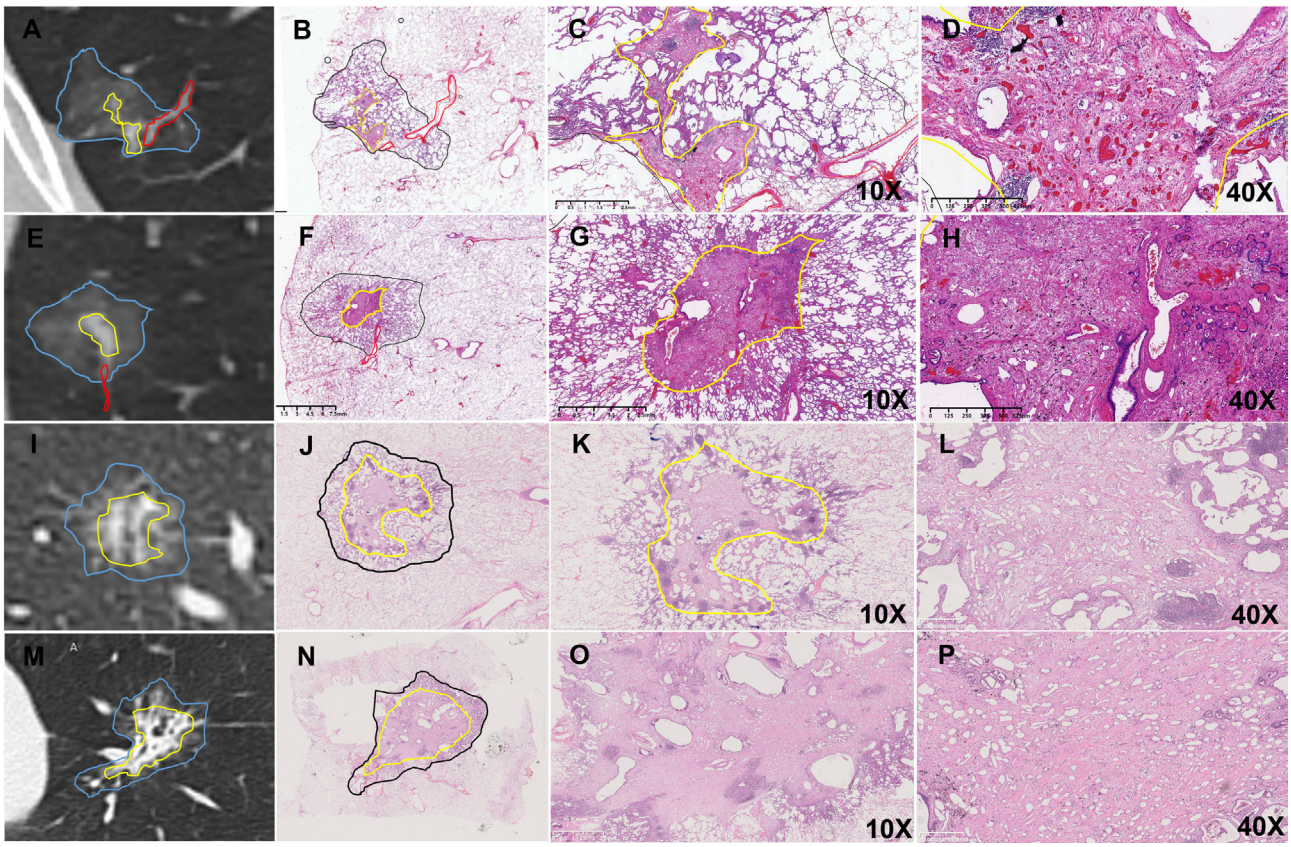

Figure S7 Presence of fibrosis in the solid component in the part-solid tumors. (A,E,I,M) The part-solid tumors on TS-CT. (B,F,J,N) The matched pathologic sections (yellow region was the radiologic solid component). (C,G,K,O) Presence of fibrosis on the pathologic sections (original magnification: ×10). (D,H,L,P) Presence of fibrosis on the pathologic sections (original magnification: ×40). TS-CT, thin-section computed tomography.

https://dx.doi.org/10.21037/tlcr-2024-1063

Table S1 Clinicopathologic features of patients with STAS (+) in this study

No.	Gender	Age	Smoking status	Surgery	Radiologic tumor size (mm)	Radiologic solid size (mm)	Pathologic tumor size (mm)	Pathologic invasive size (mm)	Subtypes	Lymphatic and nerve invasion	Pleural invasion	N	TNM staging	Mutation status
1	M	58	Non-smoker	Segmentectomy	17.8	3.7	20.9	11.3	LEP + ACN + MIP + PAP	(–)	(–)	0	IA2	TPM3-ROS1
2	F	48	Non-smoker	Lobectomy	19.4	15.4	20.4	20.4	PAP + MIP + ACN + LEP	(–)	(–)	0	IA3	EGFR E19 del
3	M	50	Smoker	Lobectomy	31.6	21.7	24.8	23.8	PAP + ACN + MIP + LEP	(–)	(–)	0	IA3	EGFR E21 L858R
4	F	52	Non-smoker	Lobectomy	18	2.9	12.2	9.8	MIP + PAP + LEP + ACN	(–)	(–)	0	IA1	FGFR1 amplification
5	M	59	Non-smoker	Segmentectomy	20.7	9.7	13.2	9.6	ACN + PAP + LEP + MIP	(–)	(–)	0	IA1	EGFR E19 del
6	M	65	Smoker	Lobectomy	42	31.7	44.4	41	ACN + LEP + PAP + SOL + MIP	(+)	(+)	N2	IIIA	EGFR E21 L858R
7	F	69	Smoker	Lobectomy	43	25.9	28.7	25	ACN + MIP + PAP + LEP	(+)	(–)	N2	IIIA	EGFR E21 L858R

ACN, acinar; LEP, lepidic; MIP, micropapillary; PAP, papillary; SOL, solid; STAS, spread through alveolar space.

https://dx.doi.org/10.21037/tlcr-2024-1063